# Sequence Dependence of the Stability of RNA Hairpin Molecules with Six Nucleotide Loops†

Christopher J. Vecenie, Catherine V. Morrow, Allison Zyra, and Martin J. Serra*

*Department of Chemistry, Allegheny College, 520 North Main Street, Meadville, Pennsylvania 16335*

*Received August 30, 2005; Revised Manuscript Received November 22, 2005*

ABSTRACT: Thermodynamic parameters are reported for hairpin formation in 1 M NaCl by RNA sequence of the types GCGXUAAUYCGC and GGUXUAAUYACC with Watson−Crick loop closure, where XY is the set of 10 possible mismatch base pairs. A nearest-neighbor analysis of the data indicates the free energy of loop formation at 37 °C varies from 3.1 to 5.1 kcal/mol. These results agree with the model previously developed [Vecenie, C. J., and Serra, M. J. (2004) *Biochemistry 43,* 11813] to predict the stability of RNA hairpin loops: $\Delta G^\circ_{37L(n)} = \Delta G^\circ_{37i(n)} + \Delta G^\circ_{37MM} - 0.8$ (if first mismatch is GA or UU) $- 0.8$ (if first mismatch is GG and loop is closed on the 5′ side by a purine). Here, $\Delta G^\circ_{37i(n)}$ is the free energy for initiating a loop of $n$ nucleotides, and $\Delta G^\circ_{37MM}$ is the free energy for the interaction of the first mismatch with the closing base pair. Thermodynamic parameters are also reported for hairpin formation in 1 M NaCl by RNA sequence of the types GACGXUAAUYUGUC and GGUXUAAUYGCC with GU base pair closure, where XY is the set of 10 possible mismatch base pairs. A nearest-neighbor analysis of the data indicates the free energy of loop formation at 37 °C varies from 3.6 to 5.3 kcal/mol. These results allow the development of a model for predicting the stability of hairpin loops closed by GU base pairs. $\Delta G^\circ_{37L(n)}$ (kcal/mol) $= \Delta G^\circ_{37i(n)} - 0.8$ (if the first mismatch is GA) $- 0.8$ (if the first mismatch is GG and the loop is closed on the 5′ side by a purine). Note that for these hairpins, the stability of the loops does not depend on $\Delta G^\circ_{37MM}$. For hairpin loops closed by GU base pairs, the $\Delta G^\circ_{37i(n)}$ values, when $n = 4$, 5, 6, 7, and 8, are 4.9, 5.0, 4.6, 5.0, and 4.8 kcal/mol, respectively. The model gives good agreement when tested against six naturally occurring hairpin sequences. Thermodynamic values for terminal mismatches adjacent to GC, GU, and UG base pairs are also reported.

The ability of RNA to both store information and carry out catalysis has led to the idea that RNA was the first molecule involved in the evolution of life (*1*). RNA still is intimately involved in all of the major information transfer events of the cell and is even the molecule responsible for peptide bond formation during protein biosynthesis (*2*). Our understanding of the roles of RNA in the cell has improved rapidly over the past decade. Central to its role in biological processes is RNA's ability to adopt a complex three-dimensional shape.

RNA can fold into a large number of secondary and tertiary structures that are responsible for its cellular roles. The principles involved in this folding have not yet been identified. However, it is clear that secondary and tertiary structure formation are linked (*3*). Insights into the formation of secondary structural motifs will, therefore, aid in understanding the formation of the three-dimensional structure of functional RNAs.

An important step in modeling RNA structure is determining its secondary structure. Several approaches are commonly used to predict RNA secondary structure. Phylogenetic analysis uses sequence comparison of RNAs with similar function to determine common structural motifs (*4*, *5*). Chemical and enzymatic probes are used to map single-stranded and double-stranded regions of RNA (*6*, *7*). Thermodynamic analysis is used to predict the most stable secondary structure of the RNA (*8*−*10*). Combining and improving these methods have made RNA structure determination more reliable (*8*, *11*, *12*).

Hairpins are an important secondary structural motif in RNA. For example, nearly 70% of *Escherichia coli* 16S rRNA bases are found in small hairpin structures. Additionally, hairpins are involved in a number of important tertiary interactions with either proteins (*13*, *14*) or RNA (*15*, *16*). The ability of hairpins to form nucleation sites for further folding of RNA depends on the stability of the hairpin motif. Understanding of the stability of RNA hairpins is, therefore, crucial to elucidating the folding pathway and ultimate three-dimensional structure of RNA.

Hairpin loop stability can be predicted using a relatively simple nearest-neighbor model (*17*−*19*). For hairpin loops with more than three nucleotides, stability has been shown to depend on the loop size, the interaction of the first mismatch with the closing base pair, and an additional stabilization term for loops where the first loop mismatch is GA, UU, or GG. The model was developed from a small set of hairpins (20 oligomers) with CG or AU closing base

† This work was supported by the Camille and Henry Dreyfus Foundation, National Science Foundation Grant MCB-0340958, and Shanbrom Funds of Allegheny College.

* To whom correspondence should be addressed. Phone: (814) 332-5356. Fax: (814) 332-2789. E-mail: mserra@allegheny.edu.

10.1021/bi051750u CCC: $33.50 
Published on Web 01/12/2006

pairs. We have previously shown that the model used to predict the stability of hairpin loops closed by GU base pairs is slightly modified (*20*) from the model described above. For hairpin loops closed with GU base pairs, the UU first mismatch is not considered to be unusually stable.

In this report, we investigate the influence of closing base pairs on the stability of RNA hairpin loops by examining sets of hairpins closed by Watson−Crick base pairs not previously studied (i.e., GC and UA) and sets of hairpins closed by GU base pairs (UG and GU). The results of this study show that the model developed previously (*19*, *21*) for predicting the stability of hairpins loops closed by Watson−Crick base pairs, CG and AU, works well for hairpins closed by all Watson−Crick pairs. However, a different model, independent of the interaction of the first mismatch with the closing base pair, was necessary for predicting the stability of hairpin loops closed by GU base pairs.

## MATERIALS AND METHODS

*RNA Synthesis and Purification.* Oligomers were synthesized on solid support using the phosphoramidite approach with the 2′-hydroxyl group protected as the *tert*-butyl dimethylsilyl ether. After ammonia and fluoride deprotection, the crude oligomer was purified by preparative TLC (55:35:10 *n*-propanol/ammonium hydroxide/water mixture) and Sep-Pak C18 (Waters) chromatography. Purities were checked by analytical TLC or HPLC (C-18) and were greater than 95%.

*Melting Curves and Data Analysis.* The buffer for the melting studies was 1 M NaCl, 10 mM cacodylic acid, and 0.5 mM EDTA (pH 7). Strand concentrations were determined from high-temperature absorbance at 280 nm. Absorbance versus temperature curves were measured at 280 or 260 nm with a heating or cooling rate of 1.0 °C/min, on a Perkin-Elmer Lambda 2S spectrophotometer as described previously (*21*). Oligomer concentrations were varied over an at least 40-fold range between 1 mM and 10 $\mu$M.

Absorbance versus temperature profiles were fit to a two-state model with sloping baselines by using a nonlinear least-squares program (*22*). For hairpin melts, this program was adapted for a unimolecular transition. Thermodynamic parameters for hairpin formation were obtained from averages of the fits of the individual melting curves. The melting temperatures for all of the hairpins were concentration-independent, indicative of a unimolecular transition. Thermodynamic parameters for duplex formation were obtained by two methods: (1) enthalpy and entropy changes from the fits of the individual melting curves were averaged, and (2) plots of the reciprocal melting temperature, $T_M^{-1}$, versus log $C_t$ gave enthalpy and entropy changes (*23*):

$$T_M^{-1} = (2.3R/\Delta H^\circ) \log C_t + \Delta S^\circ/\Delta H^\circ \qquad (1)$$

where $C_t$ is the total concentration of the oligomer. Parameters derived from the two methods agreed within 10%, consistent with the two-state model (*24*, *25*).

*Phylogenetic Analysis.* A search of phylogenetically determined RNA secondary structures (*4*) of 305 SSU rRNAs, 169 LSU rRNAs, 16 group I RNAs, and 7 group II RNAs reveals 1811 hairpin loops of six nucleotides. The loops were characterized by the closing base pair and first mismatch.

Table 1: Thermodynamic Parameters for UA Closure Hairpin Formation at 1 M NaCl[a]

A A
U U
X Y
U•A
G•C
G•C

| XY | $T_M$ (°C) | $\Delta H^\circ$ (kcal/mol) | $\Delta S^\circ$ (eu) | $\Delta G^\circ_{37L}$[b] (kcal/mol) | $\Delta G^\circ_{37}$ measd (pred)[c] (kcal/mol) |
|---|---|---|---|---|---|
| GA | 51.4 | −36.5 ± 1.7 | −112.1 ± 5.5 | −1.62 ± 0.1 | 3.5 (3.5) |
| GG[d] | 46.6 | −35.4 ± 1.7 | −110.8 ± 5.2 | −1.04 ± 0.2 | 4.0 (4.2) |
| UU[d] | 44.8 | −32.5 ± 1.5 | −102.1 ± 4.9 | −0.83 ± 0.1 | 4.3 (4.1) |
| UC | 45.3 | −25.7 ± 2.1 | −80.2 ± 6.5 | −0.71 ± 0.2 | 4.3 (4.8) |
| AC | 43.5 | −23.5 ± 1.3 | −74.3 ± 4.3 | −0.49 ± 0.1 | 4.5 (4.6) |
| CC | 40.5 | −34.0 ± 3.0 | −108.2 ± 9.6 | −0.38 ± 0.1 | 4.6 (4.8) |
| AA[e] | 40.7 | −25.9 ± 1.3 | −82.4 ± 3.9 | −0.34 ± 0.0 | 4.7 (4.4) |
| CA | 40.2 | −29.5 ± 1.9 | −94.2 ± 6.1 | −0.30 ± 0.1 | 4.7 (4.7) |
| AG | 40.1 | −28.9 ± 2.7 | −92.5 ± 8.7 | −0.29 ± 0.1 | 4.7 (4.3) |
| CU | 34.9 | −17.2 ± 2.6 | −56.0 ± 8.2 | 0.13 ± 0.1 | 5.1 (4.9) |

[a] Solutions contained 1 M NaCl, 10 mM sodium cacodylate, and 0.5 mM EDTA (pH 7). [b] Calculated $\Delta G^\circ_{37L} = \Delta G^\circ_{37(\text{measured for hairpin formation})} - \Delta G^\circ_{37(\text{stem})}$. [c] Predicted as described in the text. [d] From ref *20*. [e] From ref *17*.

## RESULTS

We have previously shown that for RNA hairpin loops closed by a CG or AU base pair, the stability of the hairpin is dependent on the interaction of the closing base pair with the first mismatch (*17*, *19*). This interaction can be approximated by the free energy increment for the interaction of the mismatch at the end of a duplex, $\Delta G^\circ_{37MM}$. Hairpins with GA, UU, or GG first mismatches were unusually stable, and to model the stability of these hairpin loops, an additional stabilization term (−0.8 kcal/mol) was included. The current model (*19*) for predicting hairpin loop stability (loops with greater than three nucleotides) is given in eq 2.

$$\Delta G^\circ_{37L(n)}\ (\text{kcal/mol}) = \Delta G^\circ_{37i(n)} + \Delta G^\circ_{37MM} - 0.8 \text{ (if the first mismatch is GA or UU)} - 0.8 \text{ (if the first mismatch is GG and the loop is closed on the 5′ side by a purine)} \qquad (2)$$

To more fully determine the role of the first mismatch and the closing base pair in the stability of hairpin loops, the complete set of hairpins with loops of six and all possible first mismatches and the remaining closing base pairs (UA, GC, GU, and UG) were prepared and the thermodynamics of hairpin formation measured by optical melting.

The measured thermodynamic parameters for the hairpins with the 10 different first mismatches with the various closing base pairs are given in Tables 1−5. The free energy change for hairpin formation ($\Delta G^\circ_{37}$) varies depending upon the first mismatch and the closing base pair. For the initial set of hairpins with GU closing base pairs (Table 3), only five of the 10 hairpins melted in a unimolecular fashion indicative of hairpin formation. The remainder either melted as a duplex or displayed multiple transitions making it impossible to

Table 2: Thermodynamic Parameters for GC Closure Hairpin Formation at 1 M NaCl[a]

**A A**
**U U**
**X Y**
**G•C**
**C•G**
**G•C**

| XY | $T_M$ (°C) | $\Delta H°$ (kcal/mol) | $\Delta S°$ (eu) | $\Delta G°_{37L}$[b] (kcal/mol) | $\Delta G°_{37}$ measd (pred)[c] (kcal/mol) |
|---|---|---|---|---|---|
| GG | 61.3 | −37.6 ± 1.5 | −112.4 ± 5.0 | −2.73 ± 0.3 | 3.1 (3.2) |
| UU | 55.7 | −40.6 ± 1.9 | −123.3 ± 5.7 | −2.31 ± 0.1 | 3.5 (3.6) |
| GA | 58.3 | −34.3 ± 2.8 | −103.6 ± 8.9 | −2.21 ± 0.1 | 3.6 (3.0) |
| UC | 52.7 | −35.7 ± 0.9 | −109.6 ± 2.7 | −1.72 ± 0.1 | 4.1 (4.2) |
| CU | 50.8 | −38.2 ± 4.2 | −117.8 ± 15.4 | −1.62 ± 0.2 | 4.2 (4.5) |
| AG | 53.4 | −29.6 ± 5.6 | −90.6 ± 16.4 | −1.49 ± 0.3 | 4.3 (4.1) |
| AC | 50.9 | −30.6 ± 3.6 | −94.3 ± 9.2 | −1.31 ± 0.3 | 4.5 (4.2) |
| AA | 56.1 | −17.5 ± 1.6 | −53.1 ± 5.6 | −1.01 ± 0.4 | 4.8 (4.3) |
| CA | 50.4 | −22.7 ± 2.1 | −70.1 ± 6.6 | −0.93 ± 0.3 | 4.9 (4.3) |
| CC | 45.8 | −27.0 ± 2.6 | −84.5 ± 7.9 | −0.74 ± 0.5 | 5.1 (4.4) |

[a] Solutions contained 1 M NaCl, 10 mM sodium cacodylate, and 0.5 mM EDTA (pH 7). [b] Calculated $\Delta G°_{37L} = \Delta G°_{37(\text{measured for hairpin formation})} - \Delta G°_{37(\text{stem})}$. [c] Predicted as described in the text.

Table 3: Thermodynamic Parameters for GU Closure Hairpin Formation at 1 M NaCl[a]

**A A**
**U U**
**X Y**
**G•U**
**C•G**
G•C

| XY | $T_M$ (°C) | $\Delta H°$ (kcal/mol) | $\Delta S°$ (eu) | $\Delta G°_{37L}$[b] (kcal/mol) | $\Delta G°_{37}$ measd (pred)[c] (kcal/mol) |
|---|---|---|---|---|---|
| GG[d] | 48.2 | −24.5 ± 6.9 | −76.4 ± 2.2 | −0.80 ± 0.1 | 3.6 (3.8) |
| GA | 40.2 | −28.5 ± 1.2 | −90.8 ± 3.7 | −0.34 ± 0.1 | 4.0 (3.8) |
| UC | 36.1 | −27.5 ± 1.7 | −88.9 ± 4.9 | 0.08 ± 0.2 | 4.5 (4.6) |
| UU[e] | 33.5 | −29.8 ± 2.6 | −97.2 ± 8.5 | 0.30 ± 0.1 | 4.7 (4.6) |
| AA | 29.7 | −17.0 ± 1.5 | −56.2 ± 4.4 | 0.41 ± 0.2 | 4.8 (4.6) |
| AG | duplex | | | | |
| AC | duplex | | | | |
| CA | duplex | | | | |
| CU | non-two-state | | | | |
| CC | non-two-state | | | | |

[a] Solutions contained 1 M NaCl, 10 mM sodium cacodylate, and 0.5 mM EDTA (pH 7). [b] Calculated $\Delta G°_{37L} = \Delta G°_{37(\text{measured for hairpin formation})} - \Delta G°_{37(\text{stem})}$. [c] Predicted as described in the text. [d] From ref *20*. [e] From ref *18*.

obtain the thermodynamic parameters for the melting transition. Therefore, an additional set of hairpins with a longer stem sequence and GU first mismatch 5′GACG/3′CUGU was measured (Table 4). All 10 of these oligomers melted in a unimolecular fashion, although the thermodynamics derived from the melting transitions were more variable (as determined by the large standard errors in the thermodynamic parameters), probably indicating the presence of a small fraction of duplex in addition to the predominant hairpin.

The stability of an RNA hairpin can be dissected into its two structural motifs, the double-helical stem and the loop. The free energy contribution of the loop can be determined by

$$\Delta G°_{37L} = \Delta G°_{37(\text{measured for hairpin formation})} - \Delta G°_{37(\text{stem})} \quad (3)$$

Table 4: Thermodynamic Parameters for GU Closure Hairpin Formation at 1 M NaCl[a]

**A A**
**U U**
**X Y**
**G•U**
**C•G**
**A•U**
**G•C**

| XY | $T_M$ (°C) | $\Delta H°$ (kcal/mol) | $\Delta S°$ (eu) | $\Delta G°_{37L}$[b] (kcal/mol) | $\Delta G°_{37}$ measd (pred)[c] (kcal/mol) |
|---|---|---|---|---|---|
| AC | 47.9 | −40.2 ± 4.4 | −125.3 ± 14.0 | −1.37 ± 0.3 | 4.2 (4.6) |
| GA | 48.4 | −35.3 ± 5.3 | −109.7 ± 16.4 | −1.25 ± 0.2 | 4.3 (3.8) |
| GG | 50.5 | −29.6 ± 3.0 | −91.4 ± 9.2 | −1.23 ± 0.2 | 4.3 (3.8) |
| CA | 48.3 | −29.8 ± 2.6 | −92.8 ± 8.0 | −1.04 ± 0.2 | 4.5 (4.6) |
| AG | 48.6 | −27.6 ± 3.6 | −85.6 ± 11.3 | −0.99 ± 0.2 | 4.6 (4.6) |
| UC | 47.2 | −29.0 ± 3.3 | −90.4 ± 10.1 | −0.92 ± 0.2 | 4.6 (4.6) |
| AA | 46.5 | −30.6 ± 3.0 | −95.8 ± 9.4 | −0.91 ± 0.1 | 4.6 (4.6) |
| UU | 46.3 | −29.0 ± 4.6 | −90.8 ± 14.4 | −0.85 ± 0.2 | 4.7 (4.6) |
| CU | 46.4 | −28.0 ± 4.4 | −87.7 ± 14.1 | −0.82 ± 0.1 | 4.7 (4.6) |
| CC | 45.2 | −29.5 ± 3.3 | −92.7 ± 10.2 | −0.76 ± 0.2 | 4.8 (4.6) |

[a] Solutions contained 1 M NaCl, 10 mM sodium cacodylate, and 0.5 mM EDTA (pH 7). [b] Calculated $\Delta G°_{37L} = \Delta G°_{37(\text{measured for hairpin formation})} - \Delta G°_{37(\text{stem})}$. [c] Predicted as described in the text.

Table 5: Thermodynamic Parameters for GC Closure Hairpin Formation at 1 M NaCl[a]

**A A**
**U U**
**X Y**
**U•G**
**G•C**
G•C

| XY | $T_M$ (°C) | $\Delta H°$ (kcal/mol) | $\Delta S°$ (eu) | $\Delta G°_{37L}$[b] (kcal/mol) | $\Delta G°_{37}$ measd (pred)[c] (kcal/mol) |
|---|---|---|---|---|---|
| GG[d] | 48.9 | −35.1 ± 1.8 | −109.0 ± 5.0 | −1.3 ± 0.1 | 4.0 (3.8) |
| UC | 46.1 | −40.5 ± 1.7 | −126.9 ± 5.1 | −1.16 ± 0.2 | 4.2 (4.6) |
| GA | 47.4 | −31.8 ± 1.9 | −99.0 ± 6.2 | −1.00 ± 0.1 | 4.3 (3.8) |
| CC | 44.2 | −32.2 ± 2.5 | −101.4 ± 8.0 | −0.73 ± 0.1 | 4.6 (4.6) |
| AC | 44.1 | −27.0 ± 2.1 | −85.3 ± 6.4 | −0.61 ± 0.1 | 4.7 (4.6) |
| CA | 42.8 | −31.3 ± 2.6 | −99.0 ± 8.0 | −0.58 ± 0.2 | 4.7 (4.6) |
| UU[d] | 42.3 | −31.2 ± 2.5 | −98.9 ± 8.4 | −0.5 ± 0.1 | 4.8 (4.6) |
| AG | 42.9 | −25.9 ± 3.8 | −81.9 ± 11.8 | −0.48 ± 0.2 | 5.3 (4.6) |
| AA[e] | 42.8 | −27.3 ± 0.1 | −86.5 ± 0.5 | −0.47 ± 0.1 | 4.8 (4.6) |
| CU | 40.7 | −23.3 ± 1.0 | −74.4 ± 3.4 | −0.28 ± 0.1 | 5.0 (4.6) |

[a] Solutions contained 1 M NaCl, 10 mM sodium cacodylate, and 0.5 mM EDTA (pH 7). [b] Calculated $\Delta G°_{37L} = \Delta G°_{37(\text{measured for hairpin formation})} - \Delta G°_{37(\text{stem})}$. [c] Predicted as described in the text. [d] From ref *18*. [e] From ref *17*.

Since each set of hairpins contains a different stem with a different stability, to compare loop stability, the free energy contribution of the loop was determined by eq 3. The results of this analysis are presented in Tables 1−5.

In the model for hairpin loop stability, $\Delta G°_{37MM}$ is approximated by the free energy of stacking the terminal mismatches at the ends of helices. While the thermodynamic parameters for all of the terminal mismatches on UA base pairs have been previously measured (*26*), only five terminal mismatches (AA, CA, GA, AG, and GG) on helices ending in GC, only two (AA and GA) on helices ending in GU, and three (AA, GA, and GG) on helices ending in UG have been determined (*8* and references therein). Therefore, the remainder of the mismatches (XY) on the appropriate base pair was measured using self-complementary oligomers

Table 6: Thermodynamic Parameters of Duplex Formation[a]

| | $T_M^{-1}$ vs log $C_t$ plots | | | | average curve fits | | | |
|---|---|---|---|---|---|---|---|---|
| sequence | $-\Delta H°$ (kal/mol) | $-\Delta S°$ (cal/mol) | $-\Delta G°$ (kal/mol) | $T_M$[b] | $-\Delta H°$ (kal/mol) | $-\Delta S°$ (cal/mol) | $-\Delta G°$ (kal/mol) | $T_M$[b] |
| UCCGGU | 44.0 ± 4.2 | 120.6 ± 13.5 | 6.6 ± 0.2 | 43.8 | 44.0 ± 3.8 | 120.5 ± 12.2 | 6.6 ± 0.2 | 43.6 |
| CCCGGU | 39.7 ± 3.1 | 105.5 ± 9.9 | 6.9 ± 0.1 | 47.2 | 36.9 ± 2.7 | 96.5 ± 8.7 | 6.9 ± 0.1 | 48.0 |
| CCCGGA | 43.8 ± 3.8 | 119.0 ± 12.2 | 6.9 ± 0.1 | 45.9 | 45.8 ± 3.4 | 125.2 ± 11.0 | 6.9 ± 0.2 | 45.8 |
| CCCGGC | 33.8 ± 3.8 | 88.0 ± 12.1 | 6.5 ± 0.3 | 44.6 | 38.8 ± 2.4 | 104.1 ± 7.9 | 6.5 ± 0.2 | 43.8 |
| UCCGGC | 36.6 ± 4.0 | 97.3 ± 13.0 | 6.4 ± 0.3 | 43.6 | 40.6 ± 3.1 | 110.1 ± 10.2 | 6.4 ± 0.2 | 43.0 |
| reference duplex | | | | | | | | |
| CCGG[c] | 34.2 | 95.6 | 4.6 | | | | | |
| CUGGCCGA | 50.7 ± 5.5 | 132.4 ± 16.6 | 9.6 ± 0.4 | 63.2 | 53.7 ± 4.4 | 141.5 ± 13.5 | 9.9 ± 0.4 | 63.2 |
| GUGGCCGA | 54.2 ± 5.2 | 143.0 ± 15.9 | 9.9 ± 0.4 | 63.1 | 53.7 ± 2.9 | 141.3 ± 8.8 | 9.9 ± 0.2 | 63.2 |
| AUGGCCGC | 58.2 ± 2.9 | 153.8 ± 8.9 | 10.5 ± 0.2 | 65.1 | 58.3 ± 2.6 | 153.9 ± 17.4 | 10.6 ± 0.7 | 65.7 |
| CUGGCCGC | 59.6 ± 4.3 | 158.1 ± 12.6 | 10.6 ± 0.3 | 64.7 | 59.2 ± 3.7 | 156.9 ± 11.4 | 10.6 ± 0.3 | 64.9 |
| UUGGCCGC | 54.5 ± 5.1 | 142.9 ± 15.4 | 10.2 ± 0.3 | 64.7 | 56.1 ± 6.3 | 147.6 ± 18.9 | 10.3 ± 0.5 | 64.8 |
| GUGGCCGG | 48.6 ± 4.3 | 125.2 ± 13.0 | 9.7 ± 0.3 | 65.3 | 52.5 ± 7.1 | 136.9 ± 20.9 | 10.1 ± 0.3 | 65.4 |
| CUGGCCGU | 51.3 ± 1.5 | 133.9 ± 4.5 | 9.7 ± 0.1 | 63.6 | 55.8 ± 3.9 | 147.7 ± 11.7 | 10.1 ± 0.3 | 63.3 |
| UUGGCCGU | 54.6 ± 4.3 | 143.9 ± 13.3 | 9.9 ± 0.3 | 63.3 | 56.1 ± 3.6 | 148.5 ± 11.0 | 10.1 ± 0.2 | 63.1 |
| reference duplex | | | | | | | | |
| UGGCCG[d] | 51.4 | 138.5 | 8.46 | | | | | |
| GGGCGCUA | 65.8 ± 2.8 | 178.8 ± 8.5 | 10.3 ± 0.2 | 60.6 | 58.7 ± 0.6 | 157.4 ± 1.7 | 9.9 ± 0.1 | 60.8 |
| CGGCGCUA | 66.2 ± 3.8 | 180.5 ± 11.6 | 10.2 ± 0.2 | 59.6 | 58.1 ± 1.4 | 156.0 ± 4.2 | 9.7 ± 0.2 | 60.2 |
| CGGCGCUC | 61.3 ± 7.2 | 166.0 ± 21.8 | 9.8 ± 0.5 | 59.5 | 61.8 ± 3.0 | 167.5 ± 8.6 | 9.9 ± 0.3 | 59.6 |
| CGGCGCUU | 62.0 ± 2.2 | 168.1 ± 6.6 | 9.8 ± 0.1 | 59.3 | 59.1 ± 2.6 | 159.3 ± 7.8 | 9.7 ± 0.2 | 59.3 |
| AGGCGCUC | 62.8 ± 4.7 | 171.6 ± 14.3 | 9.6 ± 0.3 | 57.6 | 55.4 ± 1.2 | 149.0 ± 3.5 | 9.2 ± 0.2 | 58.1 |
| UGGCGCUU | 62.7 ± 4.4 | 171.1 ± 13.5 | 9.7 ± 0.2 | 58.0 | 60.7 ± 4.7 | 164.9 ± 14.0 | 9.6 ± 0.4 | 58.2 |
| UGGCGCUC | 57.6 ± 1.0 | 156.2 ± 2.2 | 9.1 ± 0.1 | 56.8 | 55.2 ± 2.0 | 148.8 ± 6.1 | 9.1 ± 0.1 | 56.9 |
| reference duplex | | | | | | | | |
| GGCGCU[d] | 56.2 | 153.9 | 8.5 | | | | | |

[a] Solutions contained 1 M NaCl, 10 mM sodium cacodylate, and 0.5 mM EDTA (pH 7). [b] Calculated at an oligomer concentration of $10^{-4}$ M. [c] From ref *XX*. [d] From ref *24*.

(Table 6). The nearest-neighbor thermodynamic parameters for the terminal mismatches are derived from equations equivalent to (*27*)

$$\Delta G°\binom{GX}{CY} = 0.5[\Delta G°(YCCGGX) - \Delta G°(CCGG)] \quad (4)$$

Table 7 summarizes these parameters. The measured $\Delta G°_{37}$ values for the terminal mismatches are close (on average, within 0.2 kcal/mol) to the predicted values (*8*) for all of the duplexes.

Analysis of the free energy for hairpin loop formation, $\Delta G°_{37L}$, versus the free energy increment of the first mismatch, indicated that the trend was different for hairpins closed by Watson−Crick pairs and for hairpins closed by GU pairs. The trend observed for hairpins closed by CG (*21*) and AU (*19*) base pairs, where the loops with more stable first mismatches are more stable, is also true for hairpins closed by the Watson−Crick base pairs in this study (Figure 1A). When the unusually stable mismatches (see below) are omitted, a plot of the free energy change for hairpin loop formation versus the free energy increment for the first mismatch in the loop has the trend shown in Figure 1A. The slope of the best fit line gives a $\Delta G°_{37L(6)}$ of $5.2 + \Delta G°_{37MM}$ (slope of $-0.80 \pm 0.13$), where $\Delta G°_{37MM}$ is the free energy increment for the first mismatch in the loop as measured at duplex ends. The value of 5.2 for $\Delta G°_{37L(6)}$ is close to the $\Delta G°_{37i(6)}$ of 5.4 determined from the average of all measured hairpin loops of six nucleotides (*8* and references therein).

A similar analysis for the hairpin loops closed by GU base pairs displays very different behavior (Figure 1B). Analysis of the linear fit of the data indicates that the slope of the line is not significantly different from zero, $-0.054 \pm 0.292$, indicating that the free energy increment for the first mismatch does not contribute significantly to the stability of the hairpin loops closed by GU base pairs. Since no significant trend is observed, the best model for predicting the stability of hairpin loops closed by GU base pairs would be to use the average value (4.6 kcal/mol) for the hairpin loops.

For hairpin loops closed by Watson−Crick base pairs with a pyrimidine nucleotide on the 5′ side of the loop, loops with first mismatches of GA and UU were shown to be more stable (*21*). For hairpins closed by Watson−Crick base pairs with a purine nucleotide on the 5′ side of the loop, three loops display unusual stability. In addition to first mismatches of GA and UU, the GG first mismatch is also more stable than other hairpin loops. These data points are plotted in Figure 1C with the trend line from Figure 1A included for reference. As seen for the CG and AU hairpin loop closures, all five of these first mismatches, when closed by either a GC or UA base pair, are unusually stable, by an average 0.7 kcal/mol, similar to the value of 0.8 kcal/mol determined previously (*19*, *21*).

For hairpin loops closed by GU base pairs, we have previously found that UU first mismatches do not display unusual stability (*20*). Therefore, for hairpins closed by GU base pairs, only GA and GG (with a 5′ purine closing base) are considered unusually stable. These data points are plotted in Figure 1D with the trend line from Figure 1B included for reference. Again, all of these first mismatches are unusually stable by an average of 0.5 kcal/mol [if all previously measured GU closed hairpin loops with unusually stable first mismatches are included (*18*, *20*), the average is 0.6 kcal/mol]. For simplicity, we will continue to use 0.8 kcal/mol for all of the bonus values in our predictions.

Table 7: Thermodynamic Parameters for Terminal Mismatches in 1 M NaCl (pH 7)[a]

| Base pair | X ↓ | Y → | A | C | G | U |
|---|---|---|---|---|---|---|
| 5'GX 3' | | -Δ*H*° | 5.2[b] | 5.3 | 5.6[b] | |
| 3'CY 5' | A | -Δ*S*° | 13.2[b] | 13.2 | 13.9[b] | |
| | | -Δ*G*°$_{37}$ | 1.1[b] | 1.2 | 1.3[b] | |
| | | -Δ*H*° | 7.2[b] | 1.0 | | 2.2 |
| | C | -Δ*S*° | 19.6[b] | 0.2 | | 4.0 |
| | | -Δ*G*°$_{37}$ | 1.1[b] | 1.0 | | 0.9 |
| | | -Δ*H*° | 7.1[b] | | 6.2[b] | |
| | G | -Δ*S*° | 17.8[b] | | 15.1[b] | |
| | | -Δ*G*°$_{37}$ | 1.6[b] | | 1.4[b] | |
| | | -Δ*H*° | | 2.0 | | 4.6 |
| | U | -Δ*S*° | | 2.7 | | 12.5 |
| | | -Δ*G*°$_{37}$ | | 1.2 | | 1.0 |
| 5'GX 3' | | -Δ*H*° | 3.4[c] | 0.4 | 1.3 | |
| 3'UY 5' | A | -Δ*S*° | 10.0[c] | -0.8 | 1.8 | |
| | | -Δ*G*°$_{37}$ | 0.3[c] | 0.6 | 0.7 | |
| | | -Δ*H*° | 3.4 | 4.0 | | 1.9 |
| | C | -Δ*S*° | 15.4 | 9.5 | | 3.4 |
| | | -Δ*G*°$_{37}$ | 1.1 | 1.1 | | 0.9 |
| | | -Δ*H*° | 0.6[c] | | 0.9 | |
| | G | -Δ*S*° | 0.0[c] | | -3.7 | |
| | | -Δ*G*°$_{37}$ | 0.6[c] | | 0.7 | |
| | | -Δ*H*° | | 1.1 | | 2.0 |
| | U | -Δ*S*° | | 1.2 | | 3.8 |
| | | -Δ*G*°$_{37}$ | | 0.7 | | 0.8 |
| 5'UX 3' | | -Δ*H*° | 3.7[c] | 3.5 | 3.7 | |
| 3'GY 5' | A | -Δ*S*° | 9.2[c] | 8.9 | 9.0 | |
| | | -Δ*G*°$_{37}$ | 0.8[c] | 0.8 | 0.9 | |
| | | -Δ*H*° | 1.7 | 2.7 | | 0.1 |
| | C | -Δ*S*° | 3.9 | 6.4 | | -0.7 |
| | | -Δ*G*°$_{37}$ | 0.5 | 0.7 | | 0.3 |
| | | -Δ*H*° | -3.1[c] | | 1.5[c] | |
| | G | -Δ*S*° | -11.2[c] | | 2.1[c] | |
| | | -Δ*G*°$_{37}$ | 0.5[c] | | 0.8[c] | |
| | | -Δ*H*° | | 2.1 | | 2.8 |
| | U | -Δ*S*° | | 4.9 | | 7.1 |
| | | -Δ*G*°$_{37}$ | | 0.7 | | 0.6 |

[a] Δ*G*°$_{37}$ values calculated as illustrated in the text. [b] From ref *24*. [c] From ref *18*.

To test the generality of the conclusions from this work, thermodynamic parameters were also measured for six hairpins with six nucleotide loops that occur naturally in the small or large rRNAs. These results are listed in Table 8.

Figure 2 displays three orthogonal views of the *Thermus thermophilus* small ribosomal subunit. The positions of the hairpin loops are colored red. The vast majority of hairpins loops are found localized on the exterior of the subunit. These hairpin loops are not in contact with either RNA or ribosomal proteins. A few examples of kissing hairpin loops are observed, and these are circled.

A search of phylogenetically determined secondary structures of 305 SSU rRNAs, 169 LSU rRNAs, 16 group I RNAs, and 7 Group II RNAs (*4*) revealed 1181 hairpin loops of six nucleotides. The hairpin loops were divided on the basis of the closing base pair and first mismatch. The results of the search are presented in Table 9. More than 50% of the hairpins are closed by the more stable GC or CG base pairs. As noted previously, there is also a strong preference for the base on the 5′ side of the loop to be a purine (57%). Nearly 45% of the hairpins have a first GA mismatch, and more than 66% of them are closed by a CG or GU base pair. The hairpins with UU first mismatches are almost always closed by Watson−Crick pairs where the UU mismatches display unusual stability. Interestingly, for the GG first mismatches, there is almost no preference for the hairpins to be closed with the orientation of the closing base pair with the purine to the 5′ side of the loop. In total, nearly 75% of the phylogenetically determined hairpin loops have first mismatches that are unusually stable.

## DISCUSSION

The trend, in terms of the stability of the RNA hairpins closed by Watson−Crick base pairs (GC and UA) examined here (Tables 1 and 2), parallels the trend we have observed previously for hairpins closed by CG and AU base pairs (*19*, *21*). The hairpins with unusually stable first mismatches are more stable than the remaining hairpins by approximately 0.5−1 kcal/mol. The model for predicting hairpin loop stability gives excellent agreement with the measured values for the hairpins closed by UA. The average difference is less than 0.2 kcal/mol (Table 1). The model does not do as well at predicting the stability of the hairpin loops closed by GC. Here the average difference between the measured and predicted values is 0.35 kcal/mol. For the CC first mismatch, the difference between the measured and predicted values is 0.7 kcal/mol, larger than the difference observed for any of the other hairpins but still not unreasonable given the simplicity of the model. These results suggest that the simple model (*19*, *21*) developed to predict the hairpin loop stability

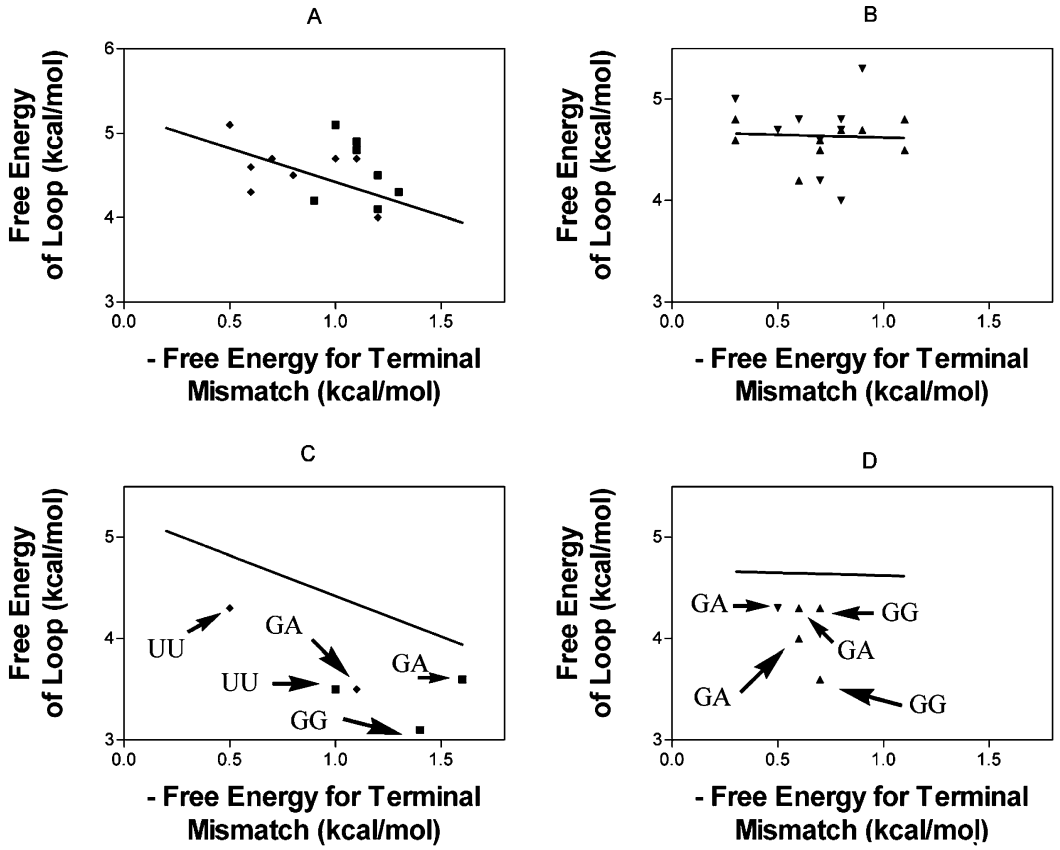


FIGURE 1: Plot of the free energy for hairpin formation. $\Delta G^\circ_{37L}$ vs the free energy increment $\Delta G^\circ_{37MM}$ for the first mismatch of the loop. Loops are closed by (◆) UA, (■) GC, (▲) GU, and (▼) UG base pairs. Panels A and C present data points excluding the unusually stable first mismatches. The solid line is the least-squares fit to the data points [note that for panel A, hairpin loops closed by CG (*21*) and AU (*19*) are included in the fit]. Panels B and D present the unusually stable first mismatch data points. The solid line is the least-squares fit to the data points in panel A or B.

for hairpins closed by Watson−Crick base pairs can be applied to a wide range of loop sequences.

The trend, in terms of the stability of the RNA hairpins closed by GU base pairs, initially appears similar to the trend observed for the Watson−Crick closed hairpins. The unusually stable hairpin loops are approximately 0.2−0.8 kcal/mol more stable than the rest (Tables 3−5). Note that for hairpins closed by GU base pairs, the UU first mismatch is not unusually stable (*20*). Closer examination (Figure 1C) of the remaining hairpins shows that the stability of the hairpin does not depend on the identity of the first mismatch. The trend line in Figure 1C is significantly different from the trend line in Figure 1A, and the slope in Figure 1C is not significantly different from zero. Therefore, the interaction of the first mismatch and the closing base pair does not contribute the stability of hairpin loops closed by GU base pairs. Thus, for these hairpins closed by GU base pairs, the stability can be predicted by using a simple penalty for the loop contribution.

Taken together, the results can be combined to develop a model for predicting the hairpin loop stability. For hairpin loops closed by Watson−Crick base pairs, the model is the same as that previously determined (*19*):

$$\Delta G^\circ_{37L(n)}\ (\text{kcal/mol}) = \Delta G^\circ_{37i(n)} + \Delta G^\circ_{37MM} - 0.8 \quad \text{(if the first mismatch is GA or UU)} - 0.8 \quad \text{(if the first mismatch is GG and the loop is closed on the 5′ side by a purine)} \quad (5)$$

While for hairpin loops closed by GU base pairs

$$\Delta G^\circ_{37L(n)}\ (\text{kcal/mol}) = \Delta G^\circ_{37i(n)} - 0.8 \quad \text{(if the first mismatch is GA)} - 0.8 \quad \text{(if the first mismatch is GG and the loop is closed on the 5′ side by a purine)} \quad (6)$$

$\Delta G^\circ_{37i(n)}$ has a value of 4.6 kcal/mol for hairpin loops of six nucleotides. Using this model, the new terminal mismatch values from Table 7, and previously measured hairpin loop stability (*17*, *18*, *20*, *28*), $\Delta G^\circ_{37i(n)}$ values for hairpin loop sizes other than six can be determined. The $\Delta G^\circ_{37i(n)}$, when $n = 4$, 5, 6, 7, and 8, are 4.9, 5.0, 4.6, 5.0, and 4.8 kcal/mol, respectively.

The model was used to predict the $\Delta G^\circ_{37L(n)}$ for the sequences listed in Tables 1−5, and the predicted values are listed in parentheses. For the 45 hairpins in Tables 1−5, only four have predicted $\Delta G^\circ_{37L(n)}$ values that are more than 0.5 kcal/mol from the observed values. The majority (30 of the 45 hairpin loops) are predicted within 0.2 kcal/mol of the actual value. The model was also used to predict the thermodynamic values for a set of naturally occurring hairpins. Comparison between the measured and predicted values is given in Table 8. While the predictions are not as accurate as those seen in Tables 1−5, there is still good agreement for most of the hairpins, in terms of both the predicted melting temperature and the free energy. The hairpin not predicted well by the model is the sequence

Table 8: Thermodynamic Parameters for Hairpin Formation of Natural Sequences in 1 M NaCl[a]

| Hairpin | $T_M$ (°C) | ΔH° (kcal/mol) | ΔS° (eu) | $\Delta G°_{37}$ (kcal/mol) | $\Delta G°_{37L}$[b] measd (kcal/mol) |
|---|---|---|---|---|---|
| CG<br>GCG A[c]<br>CGC A<br>UA | 50.2<br>(52.8) | -18.0 ± 1.2<br>(-27.6) | -55.7 ± 3.7<br>(-84.6) | -0.74 ± .13<br>(-1.32) | 5.0<br>(4.5) |
| CA<br>GGU G[d]<br>CCA G<br>UG | 55.0<br>(39.0) | -27.9 ± 2.3<br>(-22.9) | -85.0 ± 7.5<br>(-73.3) | -1.53 ± 0.24<br>(-0.15) | 3.7<br>(4.9) |
| GU<br>GGU A[e]<br>CCA A<br>AC | 54.2<br>(58.9) | -32.8 ± 3.1<br>(-25.7) | -100.0 ± 9.6<br>(-77.3) | -1.72 ± 0.20<br>(-1.55) | 3.3<br>(3.5) |
| GU<br>GGU A[f]<br>CCA A<br>AA | 51.7<br>(57.7) | -46.4 ± 9.3<br>(-25.7) | -142.9 ± 29.1<br>(-77.6) | -2.10 ± 0.42<br>(-1.55) | 3.0<br>(3.5) |
| GC<br>GGU U[g]<br>CCG U<br>GA | 57.7<br>(47.6) | -20.4 ± 2.1<br>(-23.8) | -61.6 ± 7.0<br>(-74.2) | -1.28 ± 0.23<br>(-0.72) | 4.0<br>(4.6) |
| AU<br>GCG A[h]<br>CGC U<br>CA | 47.3<br>(54.0) | -28.6 ± 5.1<br>(-30.8) | -89.2 ± 12.2<br>(-94.2) | -0.92 ± 0.29<br>(-1.6) | 4.8<br>(4.2) |

[a] Solutions contained 1 M NaCl, 10 mM sodium cacodylate, and 0.5 mM EDTA (pH 7). [b] Calculated $\Delta G°_{37L} = \Delta G°_{37(\text{measured for hairpin formation})} - \Delta G°_{37(\text{stem})}$. Values in parentheses are predicted as described in the text. [c] Sequence modeled on *Zea mays* chloroplast large rRNA position 1524. [d] Sequence modeled on *Z. mays* chloroplast large rRNA position 1524. [e] Sequence modeled on *Saccharomyces cerevisiae* large subunit rRNA position 1425. [f] Sequence modeled on *Homo sapiens* small subunit rRNA position 343. [g] Sequence modeled on *Apristurus herklotsi* large rRNA position 278. [h] Sequence modeled on *Bacillus fragilis* small rRNA 843.

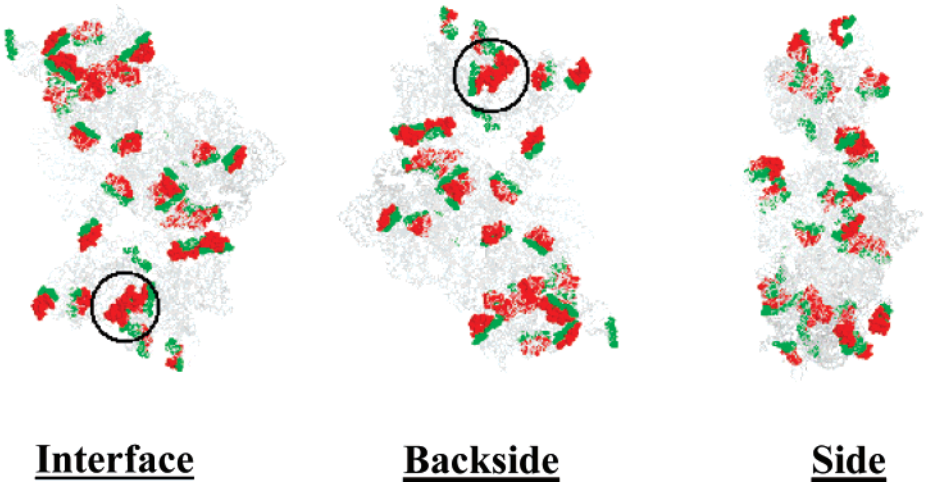


FIGURE 2: Orthogonal views of the *T. thermophilus* small ribosomal subunit (PDB entry 1FJF) highlighting the positions of hairpin loops (*29*). The nucleotides of the hairpin loops are colored red, and the closing base pairs of the loops are colored green. Examples of kissing hairpins are circled.

GGCCAGGGUACC that is more stable than predicted by 1.2 kcal/mol. The presence of three consecutive G residues in the loop may contribute to its unusual stability. The hairpin GCGCGAAAUCGC has the same first mismatch and is predicted well. The results presented here should lead to an improvement in our ability to predict the stability of RNA from sequence.

Most of the hairpin loops found in the small ribosomal subunit are localized on the exterior of the subunit where they do not interact with either RNA or protein (Figure 2).

Table 9: Percentage Occurrence of Naturally Occurring Hairpin Loops[a]

| | Closing Base Pair | | | | | | |
|---|---|---|---|---|---|---|---|
| First mismatch | GC | CG | AU | UA | GU | UG | All |
| GA | 1.9 | 17.6 | 2.1 | 1.4 | 15.1 | 6.2 | 44.4 |
| UU | 15.9 | 1.9 | 4.3 | 0.8 | 0.0 | 0.4 | 23.3 |
| GG | 4.0 | 3.2 | 1.9 | 1.3 | 0.0 | 1.4 | 11.8 |
| AA | 3.0 | 0.4 | 0.7 | 1.4 | 0.1 | 0.1 | 5.8 |
| AG | 4.0 | 0.6 | 0.1 | 1.1 | 0.0 | 0.0 | 5.8 |
| UC | 0.3 | 0.7 | 1.3 | 1.2 | 0.0 | 0.4 | 3.9 |
| CA | 0.7 | 0.6 | 0.3 | 0.1 | 0.1 | 0.1 | 1.9 |
| CU | 0.4 | 0.6 | 0.3 | 0.0 | 0.0 | 0.4 | 1.7 |
| CC | 0.1 | 0.7 | 0.0 | 0.0 | 0.0 | 0.0 | 0.8 |
| AC | 0.0 | 0.2 | 0.2 | 0.2 | 0.0 | 0.0 | 0.6 |
| All | 30.3 | 26.7 | 11.3 | 7.5 | 15.3 | 8.9 | 100.0 |

[a] Percent of phylogenetically determined hairpin loops of six nucleotides (*4*); the total number of loops with six nucleotides is 1811. Values colored red represent unusually stable first mismatches.

The primary role of hairpin loops seems to be to fold the RNA molecule so that other tertiary contact can be made. If most RNA hairpins are responsible for folding the RNA stand over on itself to form a double helix, then it would be reasonable that the most stable hairpin loops would be selected during evolution. This is exactly what is observed as nearly 75% of the hairpin loops of six nucleotides do indeed have an unusually stable first mismatch (Table 9).

## ACKNOWLEDGMENT

We thank Dr. Brent Znosko for careful reading of the manuscript.

## REFERENCES

1. Gesteland, R. F., Cech, T. R., and Atkins, J. F., Eds. (1999) *The RNA World*, 2nd ed., Cold Spring Harbor Laboratory Press, Plainview, NY.
2. Yusupov, M. M., Yusupova, G. Z., Baucom, A., Lieberman, K., Earnest, T. N., Cate, J. H., and Noller, H. F. (2001) Crystal structure of the ribosome at 5.5 Å resolution, *Science 292*, 883−896.
3. Brion, P., and Westhof, E. (1997) Hierarchy and dynamics of RNA folding, *Annu. Rev. Biophys. Biomol. Struct. 26*, 113−137.
4. Cannone, J. J., Subramanian, S., Schnare, M. N., Collett, J. R., D'Souza, L. M., Du, Y., Feng, B., Lin, N., Madabusi, L. V., Muller, K. M., Pande, N., Shang, Z., Yu, N., and Gutell, R. R. (2002) The Comparative RNA Web (CRW) Site: An online database of comparative sequence and structure information for ribosomal, intron, and other RNAs, *BMC Bioinf. 3*, 2.
5. Pace, N. R., Thomas, B. C., and Woese, C. R. (1999) Probing RNA structure, function, and history by comparative analysis, in *The RNA World* (Gesteland, R. F., Cech, T. R., and Atkins, J. F., Eds.) 2nd ed., pp 113−141, Cold Spring Harbor Laboratory Press, Plainview, NY.
6. Ehresmann, C., Baudin, F., Mougel, M., Romby, P., Ebel, J., and Ehresmann, B. (1987) Probing the structure of RNAs in solution, *Nucleic Acids Res. 15*, 9109−9128.
7. Parker, R. (1989) Genetic methods for identification and characterization of RNA-RNA and RNA-protein interactions, *Methods Enzymol. 180*, 510−517.
8. Mathews, D. H., Sabina, J., Zuker, M., and Turner, D. H. (1999) Expanded sequence dependence of thermodynamic parameters improves prediction of RNA secondary structure, *J. Mol. Biol. 288*, 911−940.
9. Rivas, E., and Eddy, S. R. (1999) A dynamic programming algorithm for RNA structure prediction including pseudoknots, *J. Mol. Biol. 285*, 2053−2068.
10. Ding, Y., and Lawrence, C. E. (2003) Statistical prediction of single-stranded regions in RNA secondary structure and application to predicting effective antisense target sites and beyond, *Nucleic Acids Res. 31*, 7280−7301.
11. Zuker, M., and Stiegler, P. (1981) Optimal computer folding of large RNA sequences using thermodynamics and auxiliary information, *Nucleic Acids Res. 9*, 133−148.
12. Mathews, D. H., Disney, M. D., Childs, J. L., Schroeder, S. J., Zuker, M., and Turner, D. H. (2004) Incorporating chemical modification constraints into a dynamic programming algorithm for prediction of RNA secondary structure, *Proc. Natl. Acad. Sci. U.S.A. 101*, 7287−7292.
13. Wu, H. N., and Uhlenbeck, O. C. (1987) Role of a bulged A residue in a specific RNA-protein interaction, *Biochemistry 26*, 8221−8227.
14. Lazinski, D., Grzadzielska, E., and Das, A. (1989) Sequence-specific recognition of RNA hairpins by bacteriophage antiterminators requires a conserved arginine-rich motif, *Cell 59*, 207−218.
15. Murphry, F. L. Wang, Y., Griffith, J. D., and Cech, T. R. (1994) Coaxially stacked RNA helices in the catalytic center of the *Tetrahymena* ribozyme, *Science 265*, 1709−1712.
16. Marino, J. P., Gregorian, R. S., Jr., Csankovski, G., and Crothers, D. M. (1995) Bent helix formation between RNA hairpins with complementary loops, *Science 268*, 1448−1454.
17. Serra, M. J., Little, M. H., Axenson, T. J., Schadt, C. A., and Turner, D. H. (1993) RNA hairpin loop stability depends on closing base pair, *Nucleic Acids Res. 21*, 3845−3849.
18. Giese, M. R., Beschart, K., Dale, T., Riley, C. K., Rowan, C., Sprouse, K. J., and Serra, M. J. (1998) Stability of RNA hairpins closed by wobble base pairs, *Biochemistry 37*, 1094−1100.
19. Vecenie, C. J., and Serra, M. J. (2004) Stability of RNA hairpin loops closed by AU base pairs, *Biochemistry 43*, 11813−11817.
20. Dale, T., Smith, R., and Serra, M. J. (2000) A test of the model to predict unusually stable RNA hairpin loop stability, *RNA 6*, 608−615.
21. Serra, M. J., Axenson, T. J., and Turner, D. H. (1994) A model for the stabilities of RNA hairpins based on a study of the sequence dependence of stability for hairpins with six nucleotides, *Biochemistry 33*, 14289−14296.
22. McDowell, J. A., and Turner, D. H. (1996) Investigation of the structural basis for thermodynamic stabilities of tandem GU mismatches: Solution structure of $(rGAG\underline{GU}CUC)_2$ by two-dimensional NMR and simulated annealing, *Biochemistry 35*, 14077−14089.
23. Borer, P., Dengler, B., and Tinoco, I., Jr. (1974) Stability of ribonucleic acid double-stranded helices, *J. Mol. Biol. 86*, 843−853.
24. Freier, S. M., Diersek, R., Jaeger, J. A., Sugimoto, N., Caruthers, M. H., Neilson, T., and Turner, D. H. (1986) Improved free-energy parameters for the predictions of RNA duplex stability, *Proc. Natl. Acad. Sci. U.S.A. 83*, 9373−9377.
25. Allawi, H. T., and SantaLucia, J., Jr. (1997) Thermodynamic and NMR of internal G•T mismatches in DNA, *Biochemistry 36*, 10581−10594.
26. Sugimoto, N., Kierzek, R., and Turner, D. H. (1987) Sequence dependence for the energetics of terminal mismatches in rbooligonucleotides, *Biochemistry 26*, 4559−4562.
27. Hickey, D. R., and Turner, D. H. (1985) Effects of terminal mismatches on RNA stability: Thermodynamics of duplex formation for ACCGGGp, ACCGGAp, and ACCGGCp, *Biochemistry 24*, 3987−3991.
28. Serra, M. J., Little, M. H., Axenson, T. J., Schadt, C. A., and Turner, D. H. (1993) RNA hairpin loop stability depends on closing base pair, *Nucleic Acids Res. 21*, 3845−3849.
29. (a) Wimberly, B. T., Brodersen, D. E., Clemons, W. M., Jr., Morgan-Warren, R. J., Carter, A. P., Vonrhein, C., Hartsch, T., and Ramakrishnan, V. (2000) Structure of the 30S ribosomal subunit, *Nature 407*, 327−339. (b) Petersheim, M., and Turner, D. H. (1983) Base-stacking and base-pairing contributions to helix stability: thermodynamics of double-helix formation with CCGG, CCGGp, CCGGAp, ACCGGp, CCGGUp, and ACCGGUp, *Biochemistry, 22*, 256−63.

BI051750U